ORGANOMETALLICS
Article
pubs.acs.org/Organometallics

Synthesis and Catalytic Hydrogenation Reactivity of a Chromium Catecholate Porous Organic Polymer

Jeffrey Camacho-Bunquin,[†] Nathan A. Siladke,[†] Guanghui Zhang,[†] Jens Niklas,[†] Oleg G. Poluektov,[†] SonBinh T. Nguyen,[†,‡] Jeffrey T. Miller,[†] and Adam S. Hock*,[†,§]

[†]Chemical Sciences and Engineering Division, Argonne National Laboratory, Argonne, Illinois 60439, United States

[‡]Department of Chemistry and International Institute for Nanotechnology, Northwestern University, Evanston, Illinois 60208, United States

[§]Department of Biological and Chemical Sciences, Illinois Institute of Technology, Chicago, Illinois 60616, United States

Supporting Information

ABSTRACT: A single-site chromium catecholate POP (catPOP A_2B_1) was synthesized and characterized via AT-IR, XAS, and EPR spectroscopy. The well-defined, four-coordinate, 11-electron Cr(III) centers bound to catecholate POP were demonstrated to be active hydrogenation catalysts for nonpolar unsaturated organic substrates under mild conditions (5 mol % of Cr, 200 psi of H_2, 60 °C). This material constitutes the first example of a well-defined, supported organometallic chromium hydrogenation precatalyst.

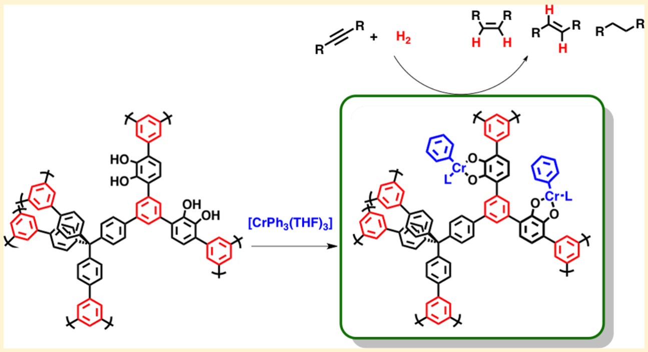

INTRODUCTION

The development of well-defined, isolated organometallic sites on solid supports continues to be an active area of research in catalysis.[1,2] Efforts in this area target practical and efficient catalyst technologies by combining the high selectivity and reactivity of molecular catalysts and the stability and ease of recovery of supported catalytic materials.[1−3] In addition, this catalyst design strategy has provided a growing number of well-defined platform compounds that are amenable to structural and rigorous mechanistic investigations, both of which are crucial elements for the rational design of functional catalysts.

Recent reports show a burgeoning interest in well-defined, isolated chromium species on polyoxygenated supports (e.g., alumina, silica) as (1) models for industrial polymerization catalyst active sites and (2) high-reactivity surface species that can activate inert bonds. The Copéret group recently reported a single-site chromium on silica catalyst that mimics the active sites in Phillips-type catalysts,[4] providing important insights into the mechanism of chromium-catalyzed olefin polymerization.[5] The group of Scott, on the other hand, successfully nucleated organometallic Cr^{4+} species on silica that catalyze alkane metathesis via C−H bond activation.[6]

Our group[7] and others[8] have recently focused on a family of transition-metal catalysts supported with catecholate-containing porous organic polymers (catPOP). These polymeric oxygenated binding sites possess several desirable properties for catalyst supports: (1) inertness toward acids, (2) porosity, and (3) tunability.[7,8] Since the reactive catecholate coordination sites are already integrated into the polymer backbone, the catPOP architecture allows for nucleation of isolated low-coordinate, monomeric species that are typically unstable in solution. In contrast to inorganic oxide supports, the bidentate catecholate site on catPOP provides a unique ligand coordination environment that can impart unique and unprecedented reactivity to low-coordinate organometallic chromium species.

While chromium has been primarily studied for polymerization[4,5,9] and oxidation catalysis,[10] its reactivity for reduction remains relatively unexplored. A few homogeneous zerovalent chromium carbonyl[11] and unstable chromium alkyl complexes[12] hydrogenate olefins after a preactivation and under forcing conditions, while a few chromium hydride species are only capable of stoichiometric reduction of a range of organic substrates.[13] We recently reported a chromium catPOP catalyst that hydrogenates olefins under mild conditions;[7e] however, complete structural assignment of the Cr active sites was unsuccessful due to the complicated reaction between catPOP and the organometallic precursor tetrakis(trimethylsilylmethyl)chromium(IV) ($[Cr(CH_2SiMe_3)_4]$). The slow and complicated metalation reaction is a consequence of (1) the low reactivity of $Cr[CH_2Si(CH_3)_3]_4$ toward protonolysis and, presumably, (2) competing Cr−alkyl decomposition pathways (i.e., α-H abstraction).[6]

Thus, we have employed the aryl chromium reagent $[CrPh_3(THF)_3]$ (**1**) as a well-defined precursor for the

Received: December 23, 2014

synthesis of a Cr catPOP catalyst. Aryl chromium complexes have been found to be far more susceptible to protonolysis and less vulnerable to Cr alkyl decomposition pathways and lead to a well-defined Cr precatalyst.[14] We report the synthesis and structural elucidation of a catPOP-supported organometallic chromium catalyst that hydrogenates nonpolar unsaturated organic substrates under mild conditions.

RESULTS AND DISCUSSION

Exposure of a red THF solution of tris(tetrahydrofuranate)-triphenylchromium(III) (**1**) to a stoichiometric amount of catPOP A_2B_1 (**2**) results in decolorization of the liquid phase to pale red, indicating the completion of the metalation reaction (Scheme 1). The reaction affords a dark brown powder, **3**, which is assigned the four-coordinate structure [(catPOP)-CrPh(L)], where L = THF, Et_2O, on the basis of the results of ligand displacement experiments, ^1H NMR, IR, X-ray absorption (XAS), and electron paramagnetic resonance (EPR) studies.

Scheme 1. Metalation Reaction between $[CrPh_3(THF)_3]$ (1) and catPOP A_2B_1 (2)

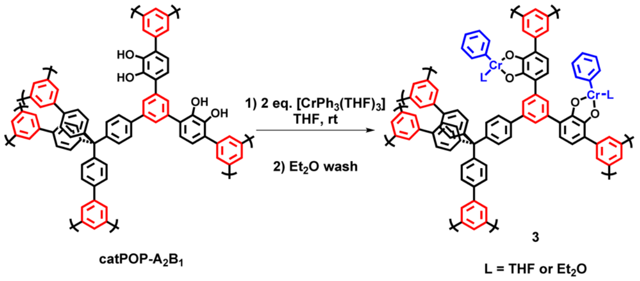

In contrast to the use of the Cr(IV) organometallic precursor $Cr[CH_2Si(CH_3)_3]_4$ (**4**) that we previously employed,[7e] **1** is an improved precursor because it reacts with catPOP **2** more quickly (2 h) at room temperature.[15] Precursor **4**, on the other hand, reacts sluggishly with A_2B_1, requiring elevated temperatures or longer metalation periods (5 days), potentially allowing for competitive chromium alkyl decomposition pathways.[6,16]

The stoichiometric metalation of catPOP **2** was confirmed in several ways. First, NMR-scale metalation experiments confirmed that a phenyl group remains bound to the Cr center in **3**, as only two of the three Cr−C(phenyl) bonds in **1** are protonated, even in the presence of a large excess of hydroxyl groups. In the presence of 1,3,5-trimethoxybenzene internal standard, the ^1H NMR scale metalation reaction showed the generation of 2 equiv of benzene (δ 7.33 ppm in THF-d_8) for every 1 equiv of **1** reacted. The presence of a Cr phenyl group in **3** is further confirmed by electron paramagnetic resonance (EPR) spectroscopy (vide infra). IR spectroscopy also shows the disappearance of the hydroxyl band at 3200 cm^{-1} that was initially present in the spectrum of **2** (Figure S1 in the Supporting Information). The IR spectrum of **3** also features very weak absorptions at 3055 and 2945 cm^{-1}, attributable to $C(sp^2)$−H and $C(sp^3)$−H bonds, respectively. The $C(sp^2)$−H bands arise from vibrations of aromatic C−H bonds of the catechol framework as well as the chromium-bound phenyl rings. The $C(sp^3)$−H band, on the other hand, is assigned to metal-bound solvent molecule(s) and any residual solvent adsorbed in the catPOP framework. This $C(sp^3)$−H IR band was also observed in the IR spectra of reported solvent-ligated metal catPOP.[7c,e]

The EPR spectrum of **3** at 10 K (Figure 1a) shows two intense signals at $g \approx 2.0$ (narrow) and $g \approx 5.0$ (broad). These EPR bands are characteristic of quartet Cr(III) centers ($S = {}^3/_2$).[17] Lower spin state chromium species arising from spin tautomerism within the chromium catecholate fragment, such as a Cr(II) semiquinoate species, were not observed. Interestingly, the $g \approx 2.0$ band was also observed in the Cr(III) catPOP species that we previously disclosed, confirming the reported Cr(III) valence state (Figure 1b).[7e] The EPR spectrum of **3** distinctively features an intense signal at $g \approx 5$, which we attribute to a Cr(III) ion bound to a carbon atom with strong covalent nature.[17f] The spectroscopic detection of a Cr−C bond is consistent with the results of the ^1H NMR scale metalation experiment where a Cr phenyl group in **1** remains unreacted. Moreover, a Cr−C EPR $g \approx 5$ signal was not observed in the previously reported Cr(III) catPOP, which had been shown to evolve all four alkyl ligands from the Cr^{4+} precursor **4**.[7e]

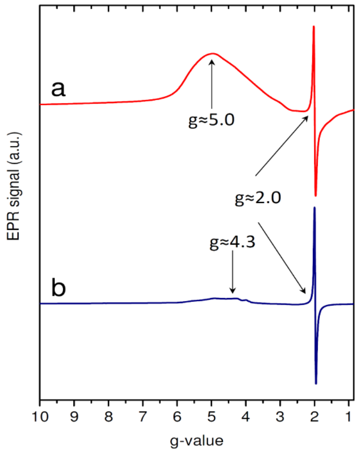

Figure 1. Continuous wave X-band EPR spectra of chromium in (a) [(catPOP)CrPh(L)] (**3**) and (b) previously reported [Cr(catPOP)].[7e] Arrows indicate low- and high-field features of the Cr(III) spectra (1 Cr per catechol loading). All spectra were recorded at T = 10 K.

The XAS pre-edge and edge energies of **3** (Figure 2) are consistent with Cr^{3+} standards (entries 4−6, Table S1 in the Supporting Information), confirming the trivalent oxidation state of Cr observed in EPR experiments. The X-ray absorption fine structure (EXAFS) data revealed a coordination number of 4.0 for the Cr^{3+} centers (Figure S5 in the Supporting Information). The observed coordination number and the

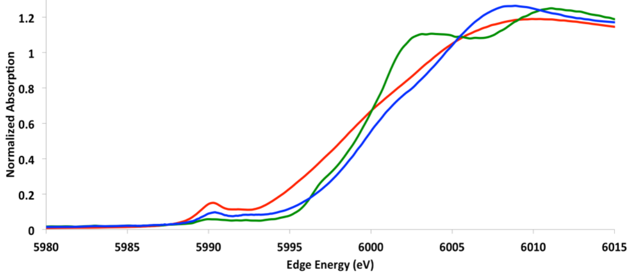

Figure 2. XAS spectra of $[CrCl_3(THF)_3]$ (**1**; green), [(catPOP)-CrPh(L)] (**3**; red), and [(catPOP)CrPh(Bipy)] (**5**; blue).

metal valence state detected via EPR and XAS support the proposed structure of an 11-electron, 4-coordinate Cr(III) center stabilized by a dianionic monocatecholate backbone, an anionic phenyl group, and one additional ligand, potentially a solvent molecule (**3** in Scheme 1).

2,2′-Bipyridine (Bipy) ligand displacement experiments were conducted (1) to identify any neutral donor molecules bound to the chromium(III) centers and (2) to evaluate the redox potential of the Cr catecholate fragment. Treatment of **3** with excess Bipy in the presence of ferrocene (internal standard for ^{1}H NMR studies) resulted in an abrupt color change to a black material, [(catPOP)CrPh(Bipy)] (**5**) (Scheme 2), and the immediate release of THF and Et_2O into the liquid phase. Approximately 1.5 equiv of ether (2/1 Et_2O/THF) for every chromium center was detected in solution upon Bipy coordination. The 1/2 equiv of ether in excess could be entrained in the catPOP cavities. The ^{1}H NMR experiment further showed that Bipy coordination is self-limiting; 1 equiv of Bipy reacts with every Cr center and the excess Bipy remained in solution over prolonged reaction periods.

Scheme 2. Ligand Displacement Reaction between [(catPOP)CrPh(L)] (3) and Bipy

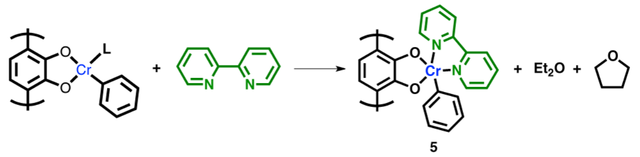

The potential reduction of Bipy by transition-metal complexes to form bipyridyl radical anion or dianion can be probed by IR spectroscopy.[18] Bipy was not reduced upon coordination with **3**, as judged by the absence of the characteristic IR bands expected for a metal-bound, reduced bipyridyl species (~900−1000 cm^{-1}; Figure S2 in the Supporting Information).[18] XAS characterization of the Bipy derivative **5** in the XANES region was also consistent with trivalent chromium upon Bipy coordination. Analysis of the EXAFS data showed an increase in the Cr coordination number from 4.0 to 4.8, consistent with the results of the NMR-scale binding experiments and a bidentate Bipy binding mode. The results of EPR, XAS, and ligand displacement experiments support the proposed structure of **5**, which features a 13-electron, 5-coordinate Cr(III) center stabilized by a dianionic catecholato ligand, an anionic phenyl group, and κ^2-coordinated Bipy molecule.

3 is a well-defined precatalyst for the hydrogenation of nonpolar unsaturated hydrocarbons under mild conditions, similar to the case for the previously reported Cr(III) cat-POP (200 psi of H_2, 60 °C).[6e] The hydrogenation activity of **3** was evaluated using diphenylacetylene (**6**) as substrate (eq 1). The summary of the results of hydrogenation catalysis experiments conducted under various conditions is presented in Table 1. At 5 mol % chromium loading (entry 1, Table 1), **3** hydrogenates diphenylacetylene to 42% substrate conversion over 6 h (TOF = 1.4 h^{-1}), affording a mixture consisting mainly of *cis*-stilbene (35%), *trans*-stilbene (1%), and the exhaustively hydrogenated product 1,2-diphenylethane (6%). The structurally undefined Cr(III) catPOP catalyst that was reported earlier[6e] exhibits higher activity under similar conditions, quantitatively hydrogenating diphenylacetylene into a mixture of 1,2-diphenylethane (81%) and *cis*-stilbene (19%) at 5 mol % Cr loading. Since the active site structure of the latter catalyst remains undefined, structure−reactivity relationship studies for both Cr(III) catPOP catalysts and mechanistic studies for the observed reactivity differences will be extremely challenging.

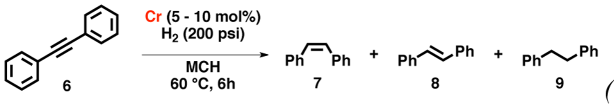

(1)

Table 1. Summary of Diphenylacetylene Hydrogenation Results

entry	cat.	amt of Cr (mol %)	time (h)	yield (%) 7	8	9	TOF (h^{-1})[a]
1	**3**	5	6	35	1	6	**1.4**
2	**3**	5	18	55	9	20	**1.0**
3	**3**	10	18	0	6	94	
4	**5**	5	6	0	0	0	
5	**5**	10	6	0	0	0	

[a]TOF is calculated as (mol of π bonds hydrogenated)/((mol of Cr) h).

The observed faster rate of alkyne hydrogenation in comparison to alkene reduction catalyzed by **3** could be attributed to the stronger binding affinity of the Cr centers for alkynes. On the other hand, the low conversion to *trans*-stilbene is an indication of low catalyst propensity to isomerize alkenes under hydrogenation conditions. Hydrogenation of diphenylacetylene under similar conditions over 18 h (entry 2, Table 1) resulted in 84% substrate conversion (TOF = 1.0 h^{-1}) into a mixture of *cis*-stilbene (55%), *trans*-stilbene (9%), and 1,2-diphenylethane (20%). A 10 mol % Cr loading (entry 3, Table 1) effected quantitative reduction into a mixture of 1,2-diphenylethane (94%) and *trans*-stilbene (6%).

The observed hydrogenation activity of **3** confirms the effectiveness of the catalyst design strategy employed: coordinatively unsaturated, monocatecholato chromium(III) is an active hydrogenation catalyst unprecedented for well-defined, freely soluble chromium complexes. A range of related homogeneous, organometallic Cr species with groups (i.e., Cr alkyl, Cr aryl) that can heterolytically activate dihydrogen have been reported in the literature; however, these species have been reported to be mainly active for olefin polymerization and oxidation.[19]

At this point it is not clear whether the catecholato ligand is key to the hydrogenation mechanism, the catPOP backbone prevents bimolecular decomposition of low-coordinate catalytic intermediates, or other factors are the source of the high activity of **3**. We attribute the surprising hydrogenation activity of the monocatecholate chromium complexes in **3** to the low coordination that is not easily achieved with soluble monocatecholate chromium species. Under hydrogenation conditions, the Cr-bound ether molecule in **3** presumably dissociates, resulting in a lower coordinate and sterically more accessible nine-electron monocatecholato Cr(III) phenyl active species. Interestingly, low-coordinate, molecular chromium aryl and chromium hydride complexes stabilized by dianionic bidentate ligands are often dimeric and coordinatively saturated, rendering them catalytically inactive. The low-coordinate nature of the active hydrogenation catalyst was further confirmed by the inactivity of the 13-electron, pentacoordinate Bipy derivative **5** for diphenylacetylene hydrogenation (entry 4, Table 1).[20]

We have not observed **3** performing hydrogenation of aromatic rings. No ring hydrogenation products were observed in the hydrogenation of 1,2-diphenylacetylene under the given conditions. Moreover, attempts to hydrogenate toluene at higher temperatures (110 °C, 150 psi H_2, 18 h) did not afford phenyl ring reduction products. These results suggest that Cr(III) is not active for aromatic hydrogenation and that metallic chromium nanoparticles are not responsible for the observed catalytic alkyne hydrogenation.[21]

One intriguing question is the precise structure of the active catalyst generated from **3**. Potential activation pathways include a nonoxidative pathway by hydrogenolysis of the Cr phenyl group, forming a Cr(III) hydride species and benzene. Alternatively, direct oxidative scission of dihydrogen by the Cr(III) centers to form a Cr(V) dihydride and cooperative chromium catecholate molecular oxidative activation of dihydrogen are alternative activation pathways. Rigorous experimental and theoretical investigation of the activation and catalytic mechanisms of **3** is currently underway.

■ SUMMARY AND CONCLUSIONS

A well-defined, POP-supported organometallic chromium precatalyst was synthesized and rigorously characterized. The hydrogenation activity displayed by Cr(III) in **3** is rare in the area of chromium catalysis, validating the catalyst design strategy that isolation of well-defined monomeric, coordinatively unsaturated transition-metal sites that are not easily formed in solution form stable catalysts for organic transformations. Spectroscopic characterization of intermediates (i.e., Cr H) and catalyst-poisoning experiments are currently underway to gain insights into the mechanism of hydrogenation and the nature of the active chromium species.

■ EXPERIMENTAL SECTION

General Considerations. All synthetic procedures and manipulations described below were carried out in a vacuum glovebox under a nitrogen atmosphere, employing rigorous glovebox and Schlenk techniques at ambient temperature unless noted otherwise. Solvents were sparged with nitrogen and dried over activated alumina. Benzene-d_6, toluene-d_8, and methylcyclohexane-d_{14} (Sigma-Aldrich) were dried over 4 Å molecular sieves and degassed using three freeze−pump−thaw cycles prior to use. Ferrocene (Sigma-Aldrich) and 1,3,5-trimethoxybenzene (Sigma-Aldrich), internal standards in NMR experiments, were used as received. Diphenylacetylene (Sigma-Aldrich) and 2,2′-bipyridine (Sigma-Aldrich) were dried in a flask with a Teflon stopcock under vacuum at ambient temperature for 16 h before use. $[CrPh_3(THF)_3]$ (**1**) was prepared on the basis of a literature procedure,[22] while catPOP A_2B_1 (**2**) was synthesized by a scaled-up modification of a reported procedure.[23] Elemental analysis was conducted by Galbraith Laboratories, Inc. (Knoxville, TN). Solution NMR experiments were conducted using a Bruker Ultra-Shield 500 MHz spectrometer (^{1}H, 500 MHz; ^{13}C, 125 MHz), and the spectra were analyzed using TopSpin (v3.1, Bruker BioSpin, Billerica, MA) and MestReNova (v6.0.2, MestreLab Research SL, Santiago de Compostela, Spain) software. Infrared (IR) spectra were collected under a nitrogen atmosphere in a glovebox using a Bruker Alpha FTIR spectrometer (Bruker Optics, Billerica, MA) with a single-reflection diamond ATR setup. Spectra at 4 cm^{-1} resolution were obtained in transmission mode over the 375−4000 cm^{-1} range. All IR data were normalized, baseline-corrected, and analyzed using OPUS (v7.0, Bruker Optics, Billerica, MA) software.

Synthesis of [(L)PhCr(catPOP) (3). To a stirred slurry of catPOP A_2B_1 (**2**; 0.497 g, 1.356 mmol in catechol) in THF (5 mL) was added a dark red solution of $[CrPh_3(THF)_3]$ (**1**; 0.835 g, 1.671 mmol) in THF (13 mL). The solution decolorized from dark red to pale red (due to unreacted excess **1**) upon stirring overnight at room temperature. The solvent was removed by filtration through a fine-porosity frit, and the insoluble metalated catPOP A_2B_1 was washed with three 10 mL portions of diethyl ether. The solid material was transferred to a vial and dried under reduced pressure for 8 h, and [(catPOP)CrPh(L)] (**3**) was isolated as a dark brown powder (0.787 g, 103%, likely due to residual solvent). IR: 3044 vw, 2978 w, 2945 w, 1705 w, 1605 m, 1500 m, 1423 s, 1391 m, 1212 m, 1116 w, 1019 s, 915 m, 877 m, 820 vs, 729 vs, 695 vs, 556 w cm^{-1}. Anal. Calcd for $C_{61}H_{48}O_6Cr_2$: C, 77.51; H, 4.81; Cr, 9.19. Found: C, 58.23; H, 5.68; Cr, 5.42. The discrepancy is most likely due to incomplete sample combustion.

^{1}H NMR Monitoring of Metalation Stoichiometry. The NMR-scale monitoring of the metalation reaction of **2** was carried out using a limiting quantity of **1**, in the presence of 1,3,5-trimethoxybenzene as internal standard. A J. Young NMR tube was charged with **2** (0.020 g, 0.055 mmol in catechol) and 0.5 mL of a THF-d_8 solution containing **1** (0.013 g, 0.025 mmol) and 1,3,5-trimethoxybenzene (0.008 g, 0.048 mmol). The reaction progress was monitored by ^{1}H NMR experiments over the course of 16 h. The reaction showed a total benzene proton integration of 12 (δ 7.33 ppm) against the expected 6 aromatic protons originating from 2 equiv of 1,3,5-trimethoxybenzene (δ 6.08 ppm), suggesting that two benzene groups are formed for every 1 equiv of **1** reacted.

^{1}H NMR Monitoring of Reaction between Bipy and 3. The NMR-scale monitoring of the ligand displacement reaction of **3** with Bipy was carried out using an excess quantity of Bipy, in the presence of ferrocene as internal standard. A J. Young NMR tube was charged with **3** (0.011 g, 0.019 mmol in catechol) and 0.5 mL of a C_6D_6 solution containing Bipy (0.007 g, 0.046 mmol) and ferrocene (0.003 g, 0.018 mmol). The reaction progress was monitored by ^{1}H NMR experiments over the course of 16 h. Approximately 1.5 equiv. of ether (2/1 Et_2O/THF) for every chromium center was detected in solution upon Bipy coordination.

Synthesis of [(catPOP)CrPh(Bipy)] (5). A solution of 2,2′-bipyridine (12.5 mg, 0.080 mmol) in THF (2 mL) was added to a stirred slurry of **3** (42 mg, 0.074 mmol) in ether (3 mL). **3** immediately turned black and was stirred at room temperature for 14 h. The solvent was removed from the reaction mixture by decantation, and the solids were washed twice with Et_2O. The final Et_2O fraction was removed in vacuo to yield [(catPOP)CrPh(Bipy)] (**5**) as a black powder (46.3 mg, 96%). IR: 3053 vw, 2935 w, 1718 w, 1602 m, 1578 w, 1497 w, 1472 m, 1443 s, 1314 w, 1222 m, 1157 w, 1107 vw, 1061 m, 1020 m, 911 m, 821 m, 763 vs, 732 s, 699 m, 653 m, 552 m cm^{-1}.

EPR Measurements. Chromium catPOP samples with various metal loadings (1%, 10%, and 100% of saturation) were used in the EPR experiments. Continuous wave (cw) X-band (9 GHz) EPR experiments were carried out with a Bruker ELEXSYS E580 EPR spectrometer (Bruker Biospin, Rheinstetten, Germany), equipped with either a super high Q resonator (Bruker ER 4122SHQE) and a helium gas flow cryostat (ICE Oxford, U.K.) or a Flexline dielectric ring resonator (Bruker EN 4118X-MD4-W1) and a helium gas flow cryostat (CF935, Oxford Instruments, U.K.). The temperature was controlled by an ITC (Oxford Instruments, U.K.). Data processing was done using Xepr (Bruker BioSpin, Rheinstetten, Germany) and Matlab 7.11.2 (The MathWorks, Inc., Natick, MA, USA)

XAS Experiments. X-ray absorption spectroscopic (XAS) experiments were conducted in the bending magnet beamline of the Materials Research Collaborative Access Team (MRCAT) at the Advanced Photon Source (APS), Argonne National Laboratory. XAS data were acquired in transmission step scan mode with photon energies selected using a water-cooled, double-crystal Si(111) monochromator. The monochromator was detuned by approximately 50%, reducing harmonic reflections. The ionization chambers were optimized for the maximum current with linear response (~10^{10} photons detected/s) with 10% absorption (30% N_2 and 70% He) in the incident ion chamber and 70% absorption (90% N_2 and 10% Ar) in the transmission detector. A Cr foil spectrum (edge energy 5989 eV) was acquired simultaneously with each measurement for energy calibration.

Each solid standard sample of [Cr(acac)$_3$], [CrCl$_3$(THF)$_3$], and [CrPh$_3$(THF)$_3$] was mixed with boron nitride to a weight ratio of about 4% with Cr, and **3** was mixed with nonmetalated catPOP A_2B_1 to a weight ratio of about 4% Cr in the glovebox. The mixture was mixed well with a mortar and pestle, and then 10−15 mg of the mixture was pressed into a cylindrical sample holder consisting of six wells with a radius of 4.0 mm, forming a self-supporting wafer. The sample holder was placed in a quartz tube (1 in. o.d., 10 in. length) sealed with Kapton windows by two Ultra-Torr fittings and then used for transmission mode measurement.

The edge energy of the X-ray absorption near-edge structure (XANES) spectrum was determined from the inflection point in the edge: i.e., the maximum in the first derivative of the XANES spectrum. The pre-edge energy was determined from the maximum of the pre-edge peak. Experimental phase shift and backscattering amplitude were used to fit the EXAFS data. Cr−O phase shift and backscattering amplitude were obtained from reference compounds: Cr(acac)$_3$ (6 Cr−O at 1.951 Å). Background removal and normalization procedures were carried out using the Athena software package using standard methods. Standard procedures based on WinXAS 3.2 software were used to extract the extended X-ray absorption fine structure (EXAFS) data. The coordination parameters were obtained by a least-squares fit in R space of the nearest-neighbor, k^2-weighted Fourier transform data.

Batch Catalyst Testing Procedures. Batch hydrogenation experiments were carried out in a home-built pressurized batch reactor with a PEEK or Meldin sample holder. The reactor was modified from the literature to connect to a pressurizable reactor head made from standard Swagelok components. The reactor head contains a gas inlet valve, a pressure readout, and a pressure relief valve (225 psi). The gas inlet consists of two-way and three-way valves in series to allow for complete purging of the gas lines without exposure of the interior of the loaded cell to air. As a safety precaution, all hydrogenation addition and heating setups were conducted in a fume hood behind a blast shield. Prior to use, the burst pressure of the PEEK or Medlin components were calculated to ensure an appropriate wall thickness was chosen based on the operating pressure. The entire setup was also pressure- and leak-tested with nitrogen.

Diphenylacetylene Hydrogenation. Loading of the reactants was carried out in a Vacuum Atmospheres glovebox under N_2. **3** (ca. 6−12 mg, 5−10 mol %) and 0.75 mL of a 0.25 M diphenylacetylene solution (0.188 mmol) in methylcyclohexane-d_{14} were placed in a sample holder equipped with a magnetic stir bar. The batch reactor was assembled in the glovebox, removed, and then attached to a hydrogen cylinder (Airgas, UHP grade). The gas lines were purged several times with hydrogen to remove air, and the reactor was pressurized to 200 psi and then degassed to 25 psi three times to remove N_2. The reactor was then pressurized to 200 psi, sealed, and heated to 60 °C in a preheated mineral oil bath behind a blast shield for 6−18 h. The reactor was then degassed to atmospheric pressure and disassembled, the reaction mixture was filtered to remove the insoluble material, and the solution was subjected to GC-MS and ^{1}H NMR analyses.

Toluene Hydrogenation. Loading of the reactants was carried out in a Vacuum Atmospheres glovebox under N_2. **3** (ca. 6 mg, 5 mol %) and 0.75 mL of a 0.25 M toluene solution (0.188 mmol) in methylcyclohexane-d_{14} were added to a sample holder equipped with a magnetic stir bar. The batch reactor was assembled in the glovebox, removed, and then attached to a hydrogen cylinder (Airgas, UHP grade). The gas lines were purged several times with hydrogen to remove air, and the reactor was pressurized to 200 psi and then degassed to 25 psi three times to remove N_2. The reactor was then pressurized to 200 psi, sealed, and heated to 60 °C in a preheated mineral oil bath behind a blast shield for 6 h. The reactor was then degassed to atmospheric pressure and disassembled, the reaction mixture was filtered to remove the insoluble material, and the solution was subjected to GC-MS and ^{1}H NMR analyses.

GC-MS and GC-FID Analysis. Gas chromatography−mass spectrometry (GC-MS) and flame ionization detection (GC-FID) were collected using a Thermo Scientific Trace GC Ultra Gas Chromograph system equipped with a Tri Plus RSH autosampler, a Thermo Scientific ISQ GC-MS detector, and an FID detector. The column used for the MS detector was an Agilent J&W DB-5 column (30 m × 0.25 mm × 0.25 μm film thickness), and the column used for the FID detector was an Agilent J&W DB-5MS column (30 m × 0.25 mm × 0.25 μm film thickness). The data were analyzed using the Thermo Xcalibur 2.2 SP1.48 software. Conversions were determined by taking the area of each peak and dividing by the overall summation.

Diphenylacetylene/*cis*-Stilbene Method. Gas chromatography was carried out using the following method: a 1 μL split injection with a split ratio of 100 run under a constant gas flow of 1 mL/min. The oven temperature profile is as follows: initial temperature 40 °C, hold for 0.5 min, ramp at 5 °C/min, final temperature 195 °C, total run time 31.50 min.

■ ASSOCIATED CONTENT

Ⓢ Supporting Information

Figures and tables giving EPR and XAS spectral data. This material is available free of charge via the Internet at http://pubs.acs.org.

■ AUTHOR INFORMATION

Corresponding Author

*E-mail for A.S.H.: ahock@iit.edu.

Notes

The authors declare no competing financial interest.

■ ACKNOWLEDGMENTS

The authors thank Dr. Kristine Tanabe for assistance in the GC analyses. This work was supported by the U.S. Department of Energy, Office of Basic Energy Sciences, Division of Chemical Sciences, Geosciences, and Biosciences, under Contract DE-AC02-06CH11357. Use of the Advanced Photon Source, an Office of Science User Facility operated for the U.S. Department of Energy (DOE) Office of Science by Argonne National Laboratory, was supported by the U.S. DOE under Contract No. DE-AC02-06CH11357. Materials Research Collaborative Access Team (MRCAT, Sector 10-BM) operations are supported by the Department of Energy and the MRCAT member institutions.

■ REFERENCES

(1) (a) Copéret, C.; Chabanas, M.; Petroff Saint-Arroman, R.; Basset, J.-M. *Angew. Chem., Int. Ed.* **2003**, *42*, 156−181. (b) Candy, J.-P.; Didillon, B.; Smith, E. L.; Shay, T. B.; Basset, J.-M. *J. Mol. Catal.* **1994**, *86*, 179−204. (c) Basset, J. M.; Lefebvre, F.; Santini, C. *Coord. Chem. Rev.* **1998**, *178−180*, 1703−1723. (d) Marks, T. J. *Acc. Chem. Res.* **1992**, *25*, 57−65.

(2) (a) Quignard, F.; Lecuyer, C.; Bougault, C.; Lefebvre, F.; Choplin, A.; Olivier, D.; Basset, J.-M. *Inorg. Chem.* **1992**, *31*, 928−930. (b) Eisen, M. S.; Marks, T. J. *Organometallics* **1992**, *11*, 3939−3941. (c) Choplin, A.; Besson, B.; D'Ornelas, L.; Sánchez-Delgado, R.; Basset, J.-M. *J. Am. Chem. Soc.* **1988**, *110*, 2783−2787. (d) Dufaud, V.; Niccolai, G. P.; Thivolle-Cazat, J.; Basset, J.-M. *J. Am. Chem. Soc.* **1995**, *117*, 4288−4294. (e) Lecuyer, C.; Quignard, F.; Choplin, A.; Olivier, D.; Basset, J.-M. *Angew. Chem., Int. Ed. Engl.* **1991**, *30*, 1660−1661. (f) Finch, W. C.; Gillespie, R. D.; Hedden, D.; Marks, T. J. *J. Am. Chem. Soc.* **1990**, *112*, 6221−6232. (g) Dahmen, K. H.; Hedden, D.; Burwell, R. L.; Marks, T. J. *Langmuir* **1988**, *4*, 1212−1214. (h) Jezequel, M.; Dufaud, V.; Ruiz-Garcia, M. J.; Carrillo-Hermosilla, F.; Neugebauer, U.; Niccolai, G. P.; Lefebvre, F.; Bayard, F.; Corker, J.; Fiddy, S.; Evans, J.; Broyer, J.-P.; Malinge, J.; Basset, J.-M. *J. Am. Chem. Soc.* **2001**, *123*, 3520−3540. (i) Blanc, F.; Copéret, C.; Thivolle-Cazat, J.; Basset, J.-M.; Lesage, A.; Emsley, L.; Sinha, A.; Schrock, R. R. *Angew. Chem., Int. Ed. Engl.* **2006**, *45*, 1216−1220. (j) Maury, O.; Lefort, L.; Vidal, V.; Thivolle-Cazat, J.; Basset, J.-M. *Angew. Chem., Int. Ed. Engl.* **1999**, *38*, 1952−1955. (k) Corker, J.; Lefebvre, F. D. R.;

Evans, J.; L cuyer, C.; Dufaud, V. R.; Quignard, F. O.; Choplin, A. S.; Basset, J. M. *Science* **1996**, *271*, 966−969. (l) Chabanas, M.; Quadrelli, E. A.; Fenet, B.; Copéret, C.; Thivolle-Cazat, J.; Basset, J.-M.; Lesage, A.; Emsley, L. *Angew. Chem.* **2001**, *113*, 4625−4628.

(3) (a) He, M. Y.; Xiong, G.; Toscano, P. J.; Burwell, R. L.; Marks, T. J. *J. Am. Chem. Soc.* **1985**, *107*, 641−652. (b) Nicholas, C. P.; Ahn, H.; Marks, T. J. *J. Am. Chem. Soc.* **2003**, *125*, 4325−4331. (c) Ahn, H.; Nicholas, C. P.; Marks, T. J. *Organometallics* **2002**, *21*, 1788−1806.

(4) Conley, M. P.; Delley, M. F.; Siddiqi, G.; Lapadula, G.; Norsic, S.; Monteil, V.; Safonova, O. V.; Copéret, C. *Angew. Chem., Int. Ed. Engl.* **2014**, *53*, 1872−1876.

(5) Delley, M. F.; Conley, M. P.; Copéret, C. *Catal. Lett.* **2014**, *144*, 805−808.

(6) (a) Amor Nait Ajjou, J.; Scott, S. L. *Organometallics* **1997**, *16*, 86−92. (b) Amor Nait Ajjou, J.; Rice, G. L.; Scott, S. L. *J. Am. Chem. Soc.* **1998**, *120*, 13436−13443.

(7) (a) Tanabe, K. K.; Siladke, N. A.; Broderick, E. M.; Kobayashi, T.; Goldston, J. F.; Weston, M. H.; Farha, O. K.; Hupp, J. T.; Pruski, M.; Mader, E. A.; Johnson, M. J. A.; Nguyen, S. T. *Chem. Sci.* **2013**, *4*, 2483−2489. (b) López-Encarnación, J. M.; Tanabe, K. K.; Johnson, M. J. A.; Jellinek, J. *Chem. Eur. J.* **2013**, *19*, 13646−13651. (c) Kraft, S. J.; Sánchez, R. H.; Hock, A. S. *ACS Catal.* **2013**, *3*, 826−830. (d) Kraft, S. J.; Zhang, G.; Childers, D.; Dogan, F.; Miller, J. T.; Nguyen, S. T.; Hock, A. S. *Organometallics* **2014**, *33*, 2517−2522. (e) Tanabe, K. T.; Ferrandon, M. S.; Siladke, N. A.; Kraft, S. J.; Zhang, G.; Niklas, J.; Poluektov, O. G.; Lopykinski, S. J.; Bunel, E. E.; Krause, T. R.; Miller, J. T.; Hock, A. S.; Nguyen, S. T. *Angew. Chem., Int. Ed.* **2014**, *126*, 12251−12254.

(8) (a) Totten, R. K.; Weston, M. H.; Park, J. K.; Farha, O. K.; Hupp, J. T.; Nguyen, S. T. *ACS Catal.* **2013**, *3*, 1454−1459. (b) Weston, M. H.; Farha, O. K.; Hauser, B. G.; Hupp, J. T.; Nguyen, S. T. *Chem. Mater.* **2012**, *24*, 1292−1296.

(9) (a) Albahily, K.; Al-Baldawi, D.; Gambarotta, S.; Koç, E.; Duchateau, R. *Organometallics* **2008**, *27*, 5943−5947. (b) MacAdams, L. A.; Buffone, G. P.; Incarvito, C. D.; Golen, J. A.; Rheingold, A. L.; Theopold, K. H. *Chem. Commun.* **2003**, 1164−1165. (c) Gibson, V. C.; Spitzmesser, S. K. *Chem. Rev.* **2003**, *103*, 283−315. (d) Alzamly, A.; Gambarotta, S.; Korobkov, I.; Murugesu, M.; Le Roy, J. J. H.; Budzelaar, P. H. M. *Inorg. Chem.* **2014**, *53*, 6073−6081. (e) Smith, K. M. *Coord. Chem. Rev.* **2006**, *250*, 1023−1021. (f) Britovsek, G.; Gibson, V. C. *Angew. Chem.* **1999**, *38*, 428−447.

(10) (a) Grzybowska, B.; Słoczyński, J.; Grabowski, R.; Wcisło, K.; Kozłowska, A.; Stoch, J.; Zieliński, J. *J. Catal.* **1998**, *178*, 687−700. (b) Rajesh, H.; Ozkan, U. S. *Ind. Eng. Chem. Res.* **1993**, *32*, 1622−1630. (c) Wang, S.; Murata, K.; Hayakawa, T.; Hamakawa, S.; Suzuki, K. *Appl. Catal. A: Gen.* **2000**, *196*, 1−8. (d) Fei, H.; Shin, J.; Meng, Y. S.; Adelhardt, M.; Sutter, J.; Meyer, K.; Cohen, S. M. *J. Am. Chem. Soc.* **2014**, *136*, 4965−4973.

(11) Thomas, T. J.; Brenner, A. *J. Mol. Catal.* **1983**, *18*, 197−202.

(12) Kramarz, W.; Kurek, S. S. *J. Mol. Catal.* **1985**, *33*, 305−310.

(13) Eisch, J. J.; Alila, J. R. *Organometallics* **2000**, *19*, 1211−1213.

(14) Jones, D. J.; Gibson, V. C.; Green, S. M.; Maddox, P. J.; White, A. J. P.; Williams, D. J. *J. Am. Chem. Soc.* **2005**, *127*, 11037−11046.

(15) Biphenyl formation due to [CrPh$_3$(THF)$_3$] (**1**) decomposition was not observed when the metalation was carried out with THF as solvent. Fast decomposition of **1**, to give biphenyl and a Cr(I) aryl complex as byproducts, was observed when the metalation was conducted in aromatic hydrocarbon solvents (e.g., benzene and toluene). This decomposition could be due to the instability of **1** in the absence of coordinating solvents such as diethyl ether and THF.

(16) Heintz, R. A.; Ostrander, R. L.; Rheingold, A. L.; Theopold, K. H. *J. Am. Chem. Soc.* **1994**, *116*, 11387−11396.

(17) (a) Bonomo, R. P.; Dibilio, A. J.; Riggi, F. *Chem. Phys.* **1991**, *151*, 323−333. (b) Bryliakov, K. P.; Lobanova, M. V.; Talsi, E. P. *J. Chem. Soc.-Dalton Trans.* **2002**, 2263−2265. (c) Downs, H. H.; Buchanan, R. M.; Pierpont, C. G. *Inorg. Chem.* **1979**, *18*, 1736−1740. (d) Fiorani, D.; Viticoli, S. *Solid State Commun.* **1979**, *32*, 889−892. (e) Pattison, D. I.; Levina, A.; Davies, M. J.; Lay, P. A. *Inorg. Chem.* **2001**, *40*, 214−217. (f) Shaham, N.; Cohen, H.; Meyerstein, D.; Bill, E. *J. Chem. Soc., Dalton Trans.* **2000**, 3082−3085.

(18) (a) Irwin, M.; Doyle, L. R.; Krämer, T.; Herchel, R.; McGrady, J. E.; Goicoechea, J. M. *Inorg. Chem.* **2012**, *51*, 12301−12312. (b) Zhou, W.; Desnoyer, A. N.; Bailey, J. A.; Patrick, B. O.; Smith, K. M. *Inorg. Chem.* **2013**, *52*, 2271−2273. (c) Scarborough, C. C.; Sproules, S.; Weyhermüller, T.; DeBeer, S.; Wieghardt, K. *Inorg. Chem.* **2011**, *50*, 12446−12462.

(19) (a) Thomas, B. J.; Noh, S. K.; Schulte, G. K.; Sendlinger, S. C.; Theopold, K. H. *J. Am. Chem. Soc.* **1991**, *113*, 893−902. (b) White, P. A.; Calabrese, J.; Theopold, K. H. *Organometallics* **1996**, *15*, 5473−5475. (c) Noh, S. K.; Heintz, R. A.; Haggerty, B. S.; Rheingold, A. L.; Theopold, K. H. *J. Am. Chem. Soc.* **1992**, *114*, 1892−1893. (d) MacAdams, L. A.; Kim, W.-K.; Liable-Sands, L. M.; Guzei, I. A.; Rheingold, A. L.; Theopold, K. H. *Organometallics* **2002**, *21*, 952−960. (e) MacAdams, L. A.; Buffone, G. P.; Incarvito, C. D.; Golen, J. A.; Rheingold, A. L.; Theopold, K. H. *Chem. Commun.* **2003**, 1164−1165. (f) MacAdams, L. A.; Buffone, G. P.; Incarvito, C. D.; Rheingold, A. L.; Theopold, K. H. *J. Am. Chem. Soc.* **2005**, *127*, 1082−1083. (g) Liang, Y.; Yap, G. P. A.; Rheingold, A. L.; Theopold, K. H. *Organometallics* **1996**, *15*, 5284−5286. (h) Theopold, K. H. *Acc. Chem. Res.* **1990**, *23*, 263−270. (i) Monillas, W. H.; Yap, G. P. A.; Theopold, K. H. *Angew. Chem., Int. Ed.* **2007**, *46*, 6692−6694.

(20) Trace amounts of benzene were observed in experiments with **5**, which suggests, though inconclusively, the hydrogenolysis of the Cr phenyl group in the Bipy derivative and the potential formation of an inactive, five-coordinate chromium hydride.

(21) (a) Lin, Y.; Finke, R. G. *Inorg. Chem.* **1994**, *33*, 4891−4910. (b) Widegren, J. A.; Finke, R. G. *J. Mol. Catal. A: Chem.* **2003**, *198*, 317−341.

(22) Herwig, W.; Zeiss, H. H. *J. Am. Chem. Soc.* **1957**, *79*, 6561.

(23) Weston, M. H.; Farha, O. K.; Hauser, B. G.; Hupp, J. T.; Nguyen, S. T. *Chem. Mater.* **2012**, *24*, 1292−1296.